

**Supplementary Information: Low temperature decoherence dynamics in
molecular spin systems using the Lindblad master equation**

Timothy J. Krogmeier,^{†,‡} Anthony W. Schlimgen,^{†,‡} and Kade

Head-Marsden^{*,†,‡}

†Department of Chemistry, Washington University in St. Louis, St. Louis, MO 61630 USA

‡Department of Chemistry, University of Minnesota, Minneapolis, MN 55455 USA

E-mail: khm@umn.edu

Details For Electronic Structure

Following previous work, the TZVP for sulfur, oxygen, carbon and hydrogen and CP(PPP) for vanadium basis sets in addition to the B3LYP exchange-correlation functional were chosen for **V1-V4** for their ability to predict the correct experimental spin density and hyperfine tensors.^{1,2} The computed spin densities for **V1-V4** are shown in Fig. 1.

Similarly, for **CuS** and **CuSe** the ANO-RCC-DZP for carbon and hydrogen and ANO-RCC-TZP for copper, sulfur and selenium basis sets with the M06L exchange-correlation functional were chosen for their ability to qualitatively reproduce the experimental spin density.³ The computed spin densities using these DFT parameters are plotted in Fig. 2. Computed spin densities at the metal center and nearest neighbor atoms are tabulated for **CuS** and **CuSe** in Table S1. **CuSe** has less spin density at the copper metal center as compared to **CuS**; consequently, the spin density at the ligand is greater in **CuSe** than in **CuS**.

Table S1: Computed spin densities for CuS and CuSe. Spin density for the S/Se ligands is only shown for one ligand; all four ligands had equivalent spin density for CuS and CuSe.

	Cu	Ligand
CuS	0.377925	0.162887
CuSe	0.311138	0.173191

V1-V4 each contain one vanadium and 12 distal hydrogen atoms. **CuS** and **CuSe** each have one copper and 8 distal hydrogen atoms. In each set of molecules, the predominant isotopes of the other nuclei are spin 0. Therefore, for each spin active nuclei hyperfine tensors were computed as an expectation value over the spin density of the system. Hyperfine tensor calculations were performed with the ORCA 5 quantum chemistry⁴ software package which computes the hyperfine tensor as a sum of three different contributions,

$$A_{HFC} = A_{iso} + A_{dip} + A_{orb}, \quad (\text{S1})$$

where A_{iso} is an isotropic term resulting from the Fermi contact interaction between an unpaired

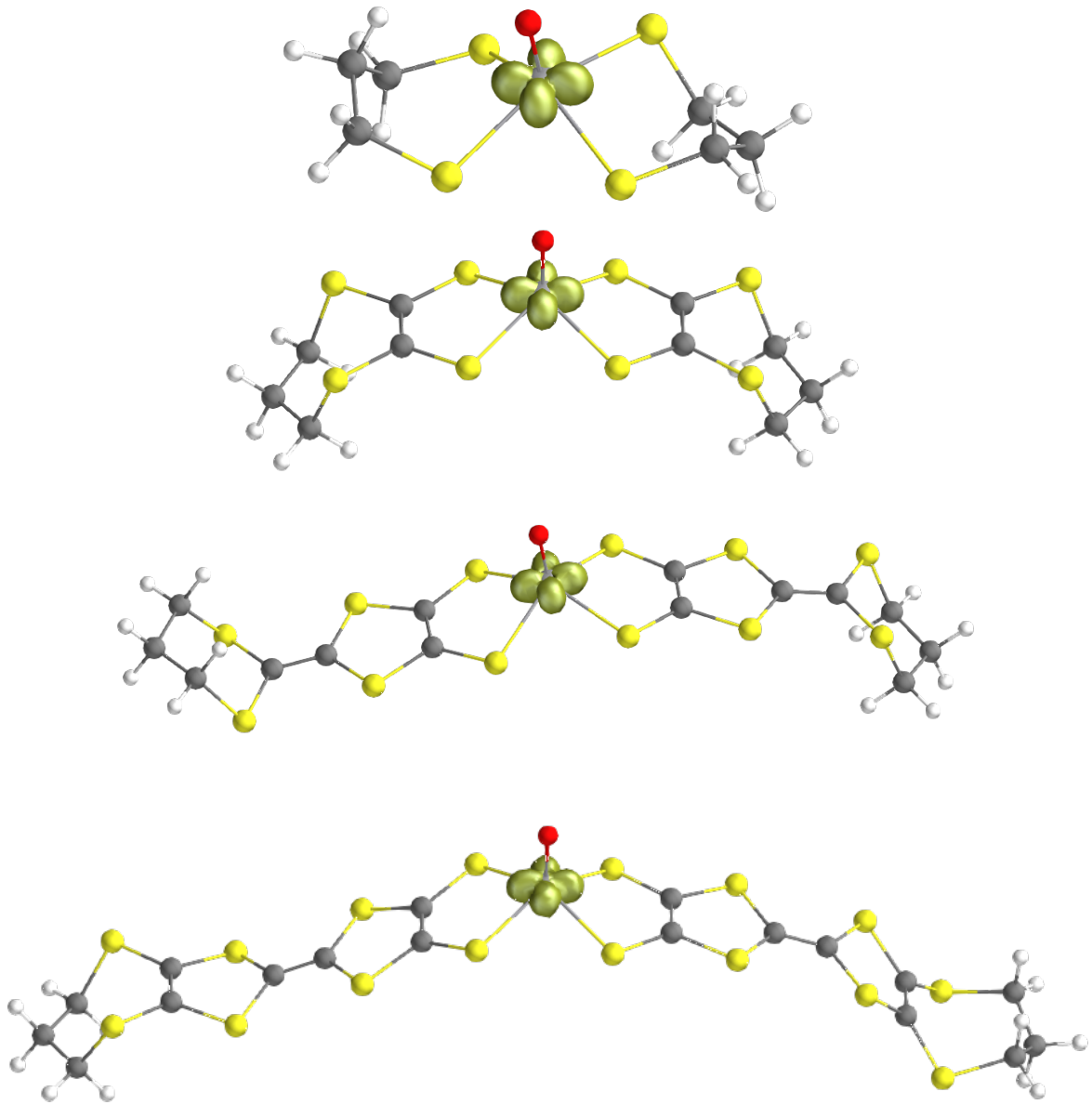


Figure 1: Spin densities computed for **V1-V4** using the B3LYP hybrid functional with a TZVP and CP(PPP) basis set. The electron is localized to the vanadium metal ion.

electron and a nucleus. A_{iso} can be written for a specific nuclear spin of interest N as

$$A_{iso,N} = \left(\frac{4}{3}\pi\langle\hat{S}_z\rangle^{-1}\right)g_eg_N\beta_e\beta_N\rho(N), \quad (\text{S2})$$

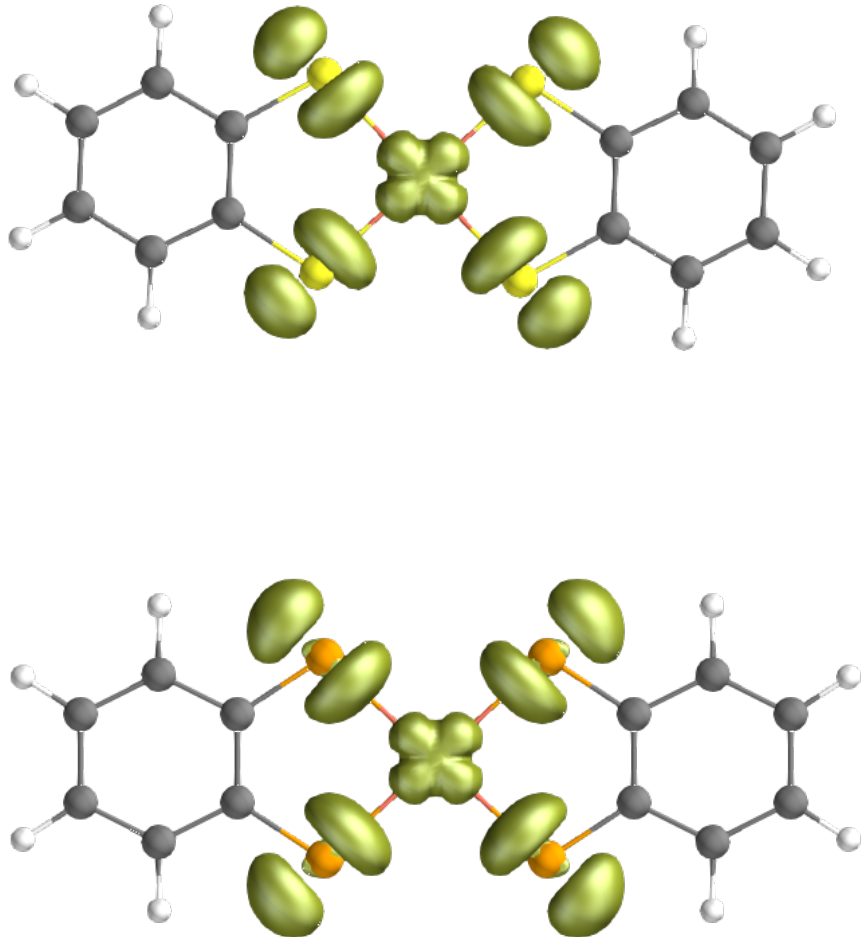


Figure 2: Spin densities computed for **CuS** (top) and **CuSe** (bottom) using the M06L functional with an ANO-RCC-DZP/TZP basis set. The electron is significantly delocalized onto the sulfur/selenium ligands.

where $\langle \hat{S}_z \rangle$ is the expectation value of the z component of the spin, $\rho(N)$ is the spin density at the nuclear spin of interest, and $g_e g_N \beta_e \beta_N$ is a proportionality factor. By considering the finite spin

density at each nuclear spin of interest, this term accounts for splitting of the nuclear energy levels via the Fermi contact interaction for nuclear spins both proximal and distal to the unpaired electron. A_{dip} is computed from

$$A_{dip,N} = P_N \sum_{i,j} \rho_{ij} \langle \psi_i | \frac{3\vec{r}_{N,\mu} \cdot \vec{r}_{N,\nu} - \delta_{\mu\nu} r_{N,e}^2}{r_{N,e}^{-5}} | \psi_j \rangle, \quad (\text{S3})$$

where P_N is the proportionality factor defined above, ρ_{ij} is the spin density matrix element, $|\psi_i\rangle$ are the basis functions, $r_{N,e}$ is the magnitude of the vector that points from the nuclear spin of interest to the electron, and $\vec{r}_{N,\mu}$ are vectors between the nuclear spin of interest to the center of the spin density for a different nucleus μ . Taking the expectation value over the spin density amounts to averaging over the spatial distribution of the electron, accurately accounting for the possibility of delocalization of the electron onto the surrounding ligands. A_{orb} is the spin-orbit coupling contribution to the hyperfine tensor, and is computed in the following way

$$A_{orb,N} = -\frac{1}{2S} P_N \sum_{i,j} \frac{\partial \rho_{ij}}{\partial I_\nu} \langle \psi_i | h_\mu^{SOC} | \psi_j \rangle, \quad (\text{S4})$$

where S and I are the spin of the electron and nucleus ν , respectively, and h_μ^{SOC} is the spin-orbit coupling operator between the basis functions $|\psi_i\rangle$. As stated above, implementation of all of these equations is done in the ORCA 5 quantum chemistry software.⁴

Using the above equations, hyperfine tensors for **V1-V4**, **CuS** and **CuSe** were computed. As an example, the hyperfine tensors for one of the most distal nuclear spins in **CuS** and **CuSe** are

$$A_{H,\text{CuS}} = \begin{pmatrix} 1.5638 & -0.0983 & 0.0002 \\ -0.0879 & 0.7295 & 0.0001 \\ 0.0001 & 0.0002 & 0.5322 \end{pmatrix}, A_{H,\text{CuSe}} = \begin{pmatrix} 1.9716 & -0.1144 & -0.0087 \\ -0.1003 & 1.0259 & 0.0036 \\ 0.0017 & -0.0361 & 0.7705 \end{pmatrix},$$

in units of MHz. The hyperfine tensor can be written as a sum of the isotropic and anisotropic

terms,

$$A_{HFC} = a_{iso} \cdot \mathbb{I} + A_{aniso}, \quad (\text{S5})$$

from which the isotropic Fermi contact constant, a_{iso} , can be extracted. a_{iso} for **CuS** is 0.9435 MHz, while for **CuSe** it is 1.2695 MHz, indicating the increased delocalization of the electron spin onto the selenium ligand is enough to alter the hyperfine tensor of the distal hydrogen nuclear spins considerably via the Fermi contact term.

Master-Equation Cluster-Correlation Expansion (ME-CCE)

To compute the dynamics of the molecular spin systems under consideration, the spin effective Hamiltonian was used,

$$\hat{H} = \hat{H}_S + \hat{H}_{int} + \hat{H}_B, \quad (\text{S6})$$

where \hat{H}_S is the system Hamiltonian, for a single unpaired electron given by

$$\hat{H}_S = -\gamma_S B \hat{S}_z, \quad (\text{S7})$$

with γ_S as the gyromagnetic ratio of the electron, B the magnitude of the external magnetic field polarized in the z -direction, and \hat{S}_z the spin operator for the electron. The bath Hamiltonian, \hat{H}_B is given by

$$\hat{H}_B = \sum_i \gamma_i B \hat{I}_i - 4 \sum_{i \neq j} I_{i,z} J_{ij} I_{j,z} + \sum_{i \neq j} J_{ij} (I_{i,+} I_{j,-} + I_{i,-} I_{j,+}), \quad (\text{S8})$$

where γ_i is the gyromagnetic ratio of nucleus i , I_i are the spin operators for nucleus i , and J_{ij} is the dipolar coupling between nuclear spins i and j . J_{ij} is defined in detail in the main text, Eq. 3.

The interaction between the electron spin and nuclear spin bath is

$$\hat{H}_{int} = \sum_i \hat{S}_z A_i \hat{I}_i, \quad (\text{S9})$$

where A is the hyperfine tensor, computed as described previously. Propagation of the density matrix by the total Hamiltonian given above allows one to obtain the density matrix at a time of interest t ,

$$\rho(t) = e^{-i\hat{H}t} \rho(0) e^{i\hat{H}t} \quad (\text{S10})$$

from which coherence of the central electron spin can be extracted by taking the partial trace over the bath nuclear spins and taking the off diagonal element of the reduced system density matrix, $\rho_S(t)$, as the coherence;

$$G(t) = \langle 0 | \rho_S(t) | 1 \rangle \quad (\text{S11})$$

For a large molecular spin system, the propagation of this Hamiltonian is not computationally tractable. The cluster-correlation expansion (CCE) approach factorizes the spin Hamiltonian into clusters of nuclear spins in their interaction with the unpaired electron in order to treat large molecular spin systems.⁵⁻⁷ In CCE, the coherence function $G(t)$ is computed by

$$G(t) = \prod_{C \subseteq \{1, 2, \dots, N\}} G_C(t), \quad (\text{S12})$$

where C is some cluster of nuclear spins in a bath of size N spins. $G_C(t)$ is defined as

$$G_C(t) = \frac{g_C}{\prod_{C' \subset C} G_{C'}}, \quad (\text{S13})$$

where g_C is computed from

$$g_C = \langle 0 | \rho_C(t) | 1 \rangle, \quad (\text{S14})$$

where $\rho_C(t)$ is obtained by taking the Hamiltonian described above and treating explicitly only the nuclear spins that are in cluster C , and averaging the remaining nuclear spins. To obtain $G_C(t)$, the contributions from all subclusters C' that are a part of C are then divided out. In the limit that $C \rightarrow N$, this becomes the exact coherence function.

The cluster contributions to g_C can be computed with a closed system propagation according

to Eq. S10, or with the Lindblad master equation, given in the main text, Eq. 1. In the latter case, the factorization is referred to as the master-equation cluster-correlation expansion (ME-CCE) approach, first implemented by Galli et al.^{8,9}

Δ Term For Each Nuclear Spin Pair

Table S2: Standard deviation of flip-flop rates for nuclear spin pairs in ensemble V1 with Δ_0 and Δ_{ij} , along with the difference between the two.

Spin Pair	Δ_{ij}	Δ_0	Difference	Spin Pair	Δ_{ij}	Δ_0	Difference
(1, 2)	0.00	0.02	-0.02	(4, 11)	0.00	0.00	-0.002
(1, 3)	0.00	0.01	-0.01	(4, 12)	0.00	0.00	-0.0026
(1, 4)	0.00	0.06	-0.06	(4, 13)	0.00	0.01	-0.0092
(1, 5)	0.00	0.01	-0.01	(5, 6)	0.44	1.33	-0.88
(1, 6)	0.00	0.02	-0.02	(5, 7)	0.01	2.49	-2.5
(1, 7)	0.00	0.01	-0.01	(5, 8)	0.00	0.00	-0.0012
(1, 8)	0.00	0.01	-0.01	(5, 9)	0.00	0.00	-0.00051
(1, 9)	0.00	0.09	-0.09	(5, 10)	0.00	0.00	-0.00024
(1, 10)	0.00	0.01	-0.01	(5, 11)	0.00	0.00	-0.00014
(1, 11)	0.00	0.01	-0.01	(5, 12)	0.00	0.00	-0.0018
(1, 12)	0.00	0.01	-0.01	(5, 13)	0.00	0.01	-0.0023
(1, 13)	0.00	0.05	-0.05	(6, 7)	27.47	101.33	-7.4e+01
(2, 3)	19.64	67.40	-47.76	(6, 8)	0.00	0.00	-0.0021
(2, 4)	0.67	1.82	-1.15	(6, 9)	0.00	0.01	-0.0029
(2, 5)	0.36	1.56	-1.20	(6, 10)	0.00	0.00	-0.003
(2, 6)	0.12	0.31	-0.20	(6, 11)	0.00	0.00	-0.002
(2, 7)	0.02	0.08	-0.06	(6, 12)	0.00	0.01	-0.0085
(2, 8)	0.00	0.00	-0.00	(6, 13)	0.02	0.05	-0.03
(2, 9)	0.00	0.01	-0.01	(7, 8)	0.00	0.00	-0.0012
(2, 10)	0.00	0.00	-0.00	(7, 9)	0.00	0.00	-0.0034
(2, 11)	0.00	0.00	-0.00	(7, 10)	0.00	0.00	-0.0017
(2, 12)	0.00	0.00	-0.00	(7, 11)	0.00	0.00	-0.0017
(2, 13)	0.00	0.00	-0.00	(7, 12)	0.01	0.01	-0.004
(3, 4)	0.08	0.84	-0.77	(7, 13)	0.00	0.02	-0.016
(3, 5)	0.74	2.38	-1.63	(8, 9)	5.20	53.97	-4.9e+01
(3, 6)	0.75	2.21	-1.47	(8, 10)	0.64	2.13	-1.5
(3, 7)	0.03	0.17	-0.14	(8, 11)	0.15	2.57	-2.4
(3, 8)	0.00	0.00	-0.00	(8, 12)	0.02	0.07	-0.05
(3, 9)	0.00	0.00	-0.00	(8, 13)	0.02	0.13	-0.11
(3, 10)	0.00	0.00	-0.00	(9, 10)	0.13	0.72	-0.59
(3, 11)	0.00	0.00	-0.00	(9, 11)	0.43	2.30	-1.9
(3, 12)	0.00	0.00	-0.00	(9, 12)	0.05	0.24	-0.2
(3, 13)	0.00	0.01	-0.00	(9, 13)	0.16	0.26	-0.1
(4, 5)	17.83	60.41	-42.58	(10, 11)	17.62	36.21	-1.9e+01
(4, 6)	0.15	0.72	-0.57	(10, 12)	0.21	1.85	-1.6
(4, 7)	0.66	1.40	-0.74	(10, 13)	0.72	3.74	-3.0
(4, 8)	0.00	0.00	-0.00	(11, 12)	0.27	2.63	-2.4
(4, 9)	0.00	0.01	-0.01	(11, 13)	0.06	1.15	-1.1
(4, 10)	0.00	0.00	-0.00	(12, 13)	9.39	77.84	-6.8e+01

Table S3: Standard deviation of flip-flop rates for nuclear spin pairs in ensemble V2 with Δ_0 and Δ_{ij} , along with the difference between the two.

Spin Pair	Δ_{ij}	Δ_0	Difference	Spin Pair	Δ_{ij}	Δ_0	Difference
(1, 2)	0.00	0.00	-0.00	(4, 11)	0.00	0.00	-1.1e-05
(1, 3)	0.00	0.00	-0.00	(4, 12)	0.00	0.00	-4.3e-05
(1, 4)	0.00	0.00	-0.00	(4, 13)	0.00	0.00	-1.1e-05
(1, 5)	0.00	0.00	-0.00	(5, 6)	1.71	2.09	-0.38
(1, 6)	0.00	0.00	-0.00	(5, 7)	0.34	0.73	-0.39
(1, 7)	0.00	0.00	-0.00	(5, 8)	0.00	0.00	-1.1e-05
(1, 8)	0.00	0.00	-0.00	(5, 9)	0.00	0.00	-4.7e-05
(1, 9)	0.00	0.00	-0.00	(5, 10)	0.00	0.00	-6.1e-06
(1, 10)	0.00	0.00	-0.00	(5, 11)	0.00	0.00	-1e-05
(1, 11)	0.00	0.00	-0.00	(5, 12)	0.00	0.00	-5.5e-05
(1, 12)	0.00	0.00	-0.00	(5, 13)	0.00	0.00	-1.2e-05
(1, 13)	0.00	0.00	-0.00	(6, 7)	37.17	62.87	-2.6e+01
(2, 3)	113.45	125.18	-11.72	(6, 8)	0.00	0.00	-6.2e-07
(2, 4)	1.69	1.95	-0.26	(6, 9)	0.00	0.00	-8.6e-06
(2, 5)	0.33	0.70	-0.37	(6, 10)	0.00	0.00	-1.5e-05
(2, 6)	0.09	0.19	-0.10	(6, 11)	0.00	0.00	-1.1e-05
(2, 7)	2.67	5.70	-3.03	(6, 12)	0.00	0.00	-5.5e-05
(2, 8)	0.00	0.00	-0.00	(6, 13)	0.00	0.00	-1.5e-05
(2, 9)	0.00	0.00	-0.00	(7, 8)	0.00	0.00	-8.1e-06
(2, 10)	0.00	0.00	-0.00	(7, 9)	0.00	0.00	-6.5e-05
(2, 11)	0.00	0.00	-0.00	(7, 10)	0.00	0.00	-5.3e-05
(2, 12)	0.00	0.00	-0.00	(7, 11)	0.00	0.00	-3.9e-05
(2, 13)	0.00	0.00	-0.00	(7, 12)	0.00	0.00	-0.0002
(3, 4)	1.72	2.77	-1.05	(7, 13)	0.00	0.00	-5.1e-05
(3, 5)	1.62	1.83	-0.22	(8, 9)	34.47	67.52	-3.3e+01
(3, 6)	0.12	0.14	-0.02	(8, 10)	1.92	2.08	-0.16
(3, 7)	0.07	0.19	-0.12	(8, 11)	1.93	2.50	-0.57
(3, 8)	0.00	0.00	-0.00	(8, 12)	0.08	0.16	-0.083
(3, 9)	0.00	0.00	-0.00	(8, 13)	0.08	0.09	-0.0094
(3, 10)	0.00	0.00	-0.00	(9, 10)	0.28	0.74	-0.46
(3, 11)	0.00	0.00	-0.00	(9, 11)	1.47	2.01	-0.54
(3, 12)	0.00	0.00	-0.00	(9, 12)	1.60	2.41	-0.81
(3, 13)	0.00	0.00	0.00	(9, 13)	0.08	0.17	-0.086
(4, 5)	33.28	44.44	-11.15	(10, 11)	26.97	47.92	-2.1e+01
(4, 6)	2.21	2.82	-0.60	(10, 12)	0.32	0.91	-0.59
(4, 7)	1.32	1.67	-0.35	(10, 13)	2.40	2.68	-0.28
(4, 8)	0.00	0.00	-0.00	(11, 12)	1.81	2.24	-0.43
(4, 9)	0.00	0.00	-0.00	(11, 13)	1.82	2.88	-1.1
(4, 10)	0.00	0.00	-0.00	(12, 13)	36.04	62.27	-2.6e+01

Table S4: Standard deviation of flip-flop rates for nuclear spin pairs in ensemble V3 with Δ_0 and Δ_{ij} , along with the difference between the two.

Spin Pair	Δ_{ij}	Δ_0	Difference	Spin Pair	Δ_{ij}	Δ_0	Difference
(1, 2)	0.00	0.00	-0.00	(4, 11)	0.00	0.00	-5e-08
(1, 3)	0.00	0.00	-0.00	(4, 12)	0.00	0.00	-2e-07
(1, 4)	0.00	0.00	-0.00	(4, 13)	0.00	0.00	-5.9e-07
(1, 5)	0.00	0.00	-0.00	(5, 6)	1.70	1.77	-0.07
(1, 6)	0.00	0.00	-0.00	(5, 7)	1.01	1.07	-0.059
(1, 7)	0.00	0.00	-0.00	(5, 8)	0.00	0.00	-5.8e-07
(1, 8)	0.00	0.00	-0.00	(5, 9)	0.00	0.00	-1.1e-07
(1, 9)	0.00	0.00	-0.00	(5, 10)	0.00	0.00	-1.3e-07
(1, 10)	0.00	0.00	-0.00	(5, 11)	0.00	0.00	-2.1e-08
(1, 11)	0.00	0.00	-0.00	(5, 12)	0.00	0.00	-1.6e-07
(1, 12)	0.00	0.00	-0.00	(5, 13)	0.00	0.00	-7.4e-07
(1, 13)	0.00	0.00	-0.00	(6, 7)	52.76	60.35	-7.6
(2, 3)	60.04	61.87	-1.82	(6, 8)	0.00	0.00	-2e-06
(2, 4)	2.49	2.50	-0.01	(6, 9)	0.00	0.00	-1e-07
(2, 5)	0.69	0.74	-0.05	(6, 10)	0.00	0.00	-1.7e-07
(2, 6)	0.13	0.15	-0.01	(6, 11)	0.00	0.00	-2.2e-07
(2, 7)	2.41	2.48	-0.08	(6, 12)	0.00	0.00	-7.7e-08
(2, 8)	0.00	0.00	-0.00	(6, 13)	0.00	0.00	-4.1e-07
(2, 9)	0.00	0.00	-0.00	(7, 8)	0.00	0.00	-5.6e-07
(2, 10)	0.00	0.00	-0.00	(7, 9)	0.00	0.00	-9.6e-07
(2, 11)	0.00	0.00	-0.00	(7, 10)	0.00	0.00	-1.1e-06
(2, 12)	0.00	0.00	-0.00	(7, 11)	0.00	0.00	-2.2e-06
(2, 13)	0.00	0.00	-0.00	(7, 12)	0.00	0.00	-8.5e-07
(3, 4)	2.63	2.65	-0.02	(7, 13)	0.00	0.00	-4.2e-07
(3, 5)	1.77	1.80	-0.02	(8, 9)	56.79	62.64	-5.9
(3, 6)	0.10	0.11	-0.00	(8, 10)	0.75	1.27	-0.51
(3, 7)	0.15	0.17	-0.02	(8, 11)	1.81	1.87	-0.064
(3, 8)	0.00	0.00	-0.00	(8, 12)	0.13	0.15	-0.024
(3, 9)	0.00	0.00	-0.00	(8, 13)	2.88	2.89	-0.014
(3, 10)	0.00	0.00	-0.00	(9, 10)	2.24	2.61	-0.37
(3, 11)	0.00	0.00	-0.00	(9, 11)	2.42	2.44	-0.022
(3, 12)	0.00	0.00	-0.00	(9, 12)	0.08	0.08	-0.00045
(3, 13)	0.00	0.00	-0.00	(9, 13)	0.14	0.18	-0.04
(4, 5)	46.27	47.55	-1.28	(10, 11)	48.78	50.55	-1.8
(4, 6)	2.92	2.94	-0.02	(10, 12)	1.78	1.92	-0.14
(4, 7)	2.13	2.15	-0.01	(10, 13)	0.87	0.95	-0.075
(4, 8)	0.00	0.00	-0.00	(11, 12)	2.49	2.51	-0.022
(4, 9)	0.00	0.00	-0.00	(11, 13)	2.16	2.17	-0.013
(4, 10)	0.00	0.00	-0.00	(12, 13)	61.96	81.37	-1.9e+01

Table S5: Standard deviation of flip-flop rates for nuclear spin pairs in ensemble V4 with Δ_0 and Δ_{ij} , along with the difference between the two.

Spin Pair	Δ_{ij}	Δ_0	Difference	Spin Pair	Δ_{ij}	Δ_0	Difference
(1, 2)	0.00	0.00	-0.00	(4, 11)	0.00	0.00	-4.2e-08
(1, 3)	0.00	0.00	-0.00	(4, 12)	0.00	0.00	-5.3e-08
(1, 4)	0.00	0.00	-0.00	(4, 13)	0.00	0.00	-6.6e-08
(1, 5)	0.00	0.00	-0.00	(5, 6)	1.70	1.70	-0.0011
(1, 6)	0.00	0.00	-0.00	(5, 7)	0.72	0.76	-0.041
(1, 7)	0.00	0.00	-0.00	(5, 8)	0.00	0.00	-1.8e-07
(1, 8)	0.00	0.00	-0.00	(5, 9)	0.00	0.00	-1.3e-07
(1, 9)	0.00	0.00	-0.00	(5, 10)	0.00	0.00	-6.5e-08
(1, 10)	0.00	0.00	-0.00	(5, 11)	0.00	0.00	-7.2e-08
(1, 11)	0.00	0.00	-0.00	(5, 12)	0.00	0.00	-6.4e-08
(1, 12)	0.00	0.00	-0.00	(5, 13)	0.00	0.00	-9.3e-08
(1, 13)	0.00	0.00	-0.00	(6, 7)	93.47	95.49	-2.0
(2, 3)	46.39	47.57	-1.18	(6, 8)	0.00	0.00	-9.3e-08
(2, 4)	1.62	1.60	0.02	(6, 9)	0.00	0.00	-5.6e-08
(2, 5)	0.79	0.80	-0.01	(6, 10)	0.00	0.00	-2.7e-08
(2, 6)	0.14	0.16	-0.02	(6, 11)	0.00	0.00	-1.6e-08
(2, 7)	2.11	2.26	-0.14	(6, 12)	0.00	0.00	-3.6e-09
(2, 8)	0.00	0.00	-0.00	(6, 13)	0.00	0.00	-3.2e-08
(2, 9)	0.00	0.00	-0.00	(7, 8)	0.00	0.00	-9.2e-08
(2, 10)	0.00	0.00	-0.00	(7, 9)	0.00	0.00	-4.4e-08
(2, 11)	0.00	0.00	-0.00	(7, 10)	0.00	0.00	-2.3e-08
(2, 12)	0.00	0.00	-0.00	(7, 11)	0.00	0.00	9.7e-10
(2, 13)	0.00	0.00	-0.00	(7, 12)	0.00	0.00	-1.8e-08
(3, 4)	2.45	2.45	-0.00	(7, 13)	0.00	0.00	-4.6e-08
(3, 5)	2.02	2.09	-0.07	(8, 9)	63.30	67.35	-4.1
(3, 6)	0.08	0.08	-0.00	(8, 10)	0.17	0.19	-0.024
(3, 7)	0.16	0.17	-0.00	(8, 11)	0.10	0.10	-0.0033
(3, 8)	0.00	0.00	-0.00	(8, 12)	2.25	2.24	0.0062
(3, 9)	0.00	0.00	-0.00	(8, 13)	1.61	1.74	-0.13
(3, 10)	0.00	0.00	-0.00	(9, 10)	3.40	3.46	-0.063
(3, 11)	0.00	0.00	-0.00	(9, 11)	0.15	0.17	-0.016
(3, 12)	0.00	0.00	-0.00	(9, 12)	2.03	2.16	-0.13
(3, 13)	0.00	0.00	-0.00	(9, 13)	0.78	0.81	-0.027
(4, 5)	74.97	78.35	-3.38	(10, 11)	50.98	54.84	-3.9
(4, 6)	2.95	3.09	-0.14	(10, 12)	1.76	1.81	-0.052
(4, 7)	1.52	1.52	0.01	(10, 13)	0.71	0.71	-0.0085
(4, 8)	0.00	0.00	-0.00	(11, 12)	3.45	3.46	-0.018
(4, 9)	0.00	0.00	-0.00	(11, 13)	2.01	2.05	-0.042
(4, 10)	0.00	0.00	-0.00	(12, 13)	47.91	48.04	-0.13

Fitting Function for Simulated Data

The fitting function used to extract T_2 decay constants from spin dynamics simulations is given by

$$C(\tau) = A(1 - B\cos(\omega\tau + d)\exp(\frac{-\tau}{T_{osc}}))\exp(-(\frac{2\tau}{T_2})^q), \quad (\text{S15})$$

where A is the amplitude of oscillation, B is the amplitude of the underlying oscillations, ω is the frequency of the underlying oscillations, τ is the time during the propagation, d is a phase factor, T_2 the overall decay constant, T_{osc} the decay constant for the underlying oscillations, and q is the stretch factor of the exponential decay.^{2,10}

References

- (1) Chen, J.; Hu, C.; Stanton, J. F.; Hill, S.; Cheng, H.-P.; Zhang, X.-G. Decoherence in Molecular Electron Spin Qubits: Insights from Quantum Many-Body Simulations. *The Journal of Physical Chemistry Letters* **2020**, *11*, 2074–2078.
- (2) Graham, M. J.; Yu, C.-J.; Krzyaniak, M. D.; Wasielewski, M. R.; Freedman, D. E. Synthetic Approach To Determine the Effect of Nuclear Spin Distance on Electronic Spin Decoherence. *Journal of the American Chemical Society* **2017**, *139*, 3196–3201.
- (3) Fataftah, M. S.; Krzyaniak, M. D.; Vlaisavljevich, B.; Wasielewski, M. R.; Zadrozny, J. M.; Freedman, D. E. Metal–ligand covalency enables room temperature molecular qubit candidates. *Chemical Science* **2019**, *10*, 6707–6714.
- (4) Neese, F.; Wennmohs, F.; Becker, U.; Ripplinger, C. The ORCA quantum chemistry program package. *The Journal of Chemical Physics* **2020**, *152*.
- (5) Yang, W.; Liu, R.-B. Quantum many-body theory of qubit decoherence in a finite-size spin bath. *Physical Review B* **2008**, *78*, 085315.
- (6) Zhao, N.; Ho, S.-W.; Liu, R.-B. Decoherence and dynamical decoupling control of nitrogen vacancy center electron spins in nuclear spin baths. *Physical Review B* **2012**, *85*, 115303.
- (7) Yang, Z.-S.; Wang, Y.-X.; Tao, M.-J.; Yang, W.; Zhang, M.; Ai, Q.; Deng, F.-G. Longitudinal relaxation of a nitrogen-vacancy center in a spin bath by generalized cluster-correlation expansion method. *Annals of Physics* **2020**, *413*, 168063.
- (8) Onizhuk, M.; Wang, Y.-X.; Nagura, J.; Clerk, A. A.; Galli, G. Understanding Central Spin Decoherence Due to Interacting Dissipative Spin Baths. *Physical Review Letters* **2024**, *132*, 250401.
- (9) Onizhuk, M.; Galli, G. PyCCE: A Python Package for Cluster Correlation Expansion Simulations of Spin Qubit Dynamics. *Advanced Theory and Simulations* **2021**, *4*, 2100254.

- (10) Huber, M.; Lindgren, M.; Hammarström, P.; Mårtensson, L.-G.; Carlsson, U.; Eaton, G. R.; Eaton, S. S. Phase memory relaxation times of spin labels in human carbonic anhydrase II: pulsed EPR to determine spin label location. *Biophysical chemistry* **2001**, *94*, 245–256.